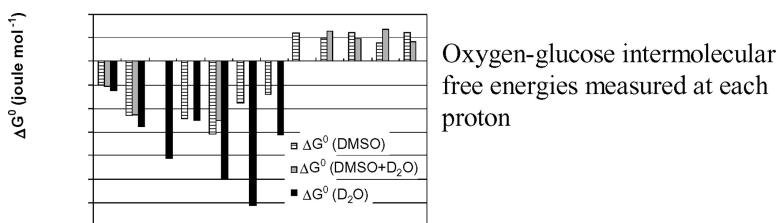


Local Measures of Intermolecular Free Energies in Solution

Ching-Ling Teng, Silvia Martini, and Robert G. Bryant

J. Am. Chem. Soc., **2004**, 126 (46), 15253-15257 • DOI: 10.1021/ja0462528 • Publication Date (Web): 02 November 2004

Downloaded from <http://pubs.acs.org> on April 5, 2009



More About This Article

Additional resources and features associated with this article are available within the HTML version:

- Supporting Information
- Links to the 1 articles that cite this article, as of the time of this article download
- Access to high resolution figures
- Links to articles and content related to this article
- Copyright permission to reproduce figures and/or text from this article

[View the Full Text HTML](#)

Local Measures of Intermolecular Free Energies in Solution

Ching-Ling Teng,[†] Silvia Martini,[§] and Robert G. Bryant^{*.†.‡}

Contribution from the Chemistry Department and Biophysics Program, University of Virginia, Charlottesville, Virginia 22904, and Department of Chemical and Biosystems Sciences, University of Siena, Via A. Moro 2, 53100 Siena, Italy

Received June 24, 2004; E-mail: rgb4g@virginia.edu

Abstract: Proton spin–lattice relaxation rate changes induced by freely diffusing oxygen in aqueous and mixed solvents are reported for representative amino acids and glucose. The local oxygen concentration at each spectrally resolved proton was deduced from the paramagnetic contribution to the relaxation rate. The measured relaxation increment is compared to that of the force-free diffusion relaxation model, and the differences are related to a free energy for the oxygen association with different portions of the solute molecules. The free energy differences are small, on the order of -800 to -2000 J/mol, but are uniformly negative for all proton positions measured on the amino acids in water and reflect the energetic benefit of weak association of hydrophobic cosolutes. For glucose, CH proton positions report negative free energies for oxygen association, the magnitude of which depends on the solvent; however, the hydroxyl positions report positive free energy differences relative to the force-free diffusion model, which is consistent with partial occupancy in the OH region by a solvent hydrogen bond.

The energetics of intermolecular contacts is central to chemical reactivity and molecular recognition. The details of intermolecular exploration impact both the thermodynamics and the kinetics of reactions in condensed phases and are central to a number of efforts to control catalytic processes ranging from heterogeneous inorganic systems to crucial enzymic components of biological processes. The definition of the nature of intermolecular contact is difficult, although molecular simulations provide one powerful approach to the problem.¹ Experimental approaches have predominantly rested on spectroscopic techniques that may provide structural or spatial resolution within the interacting molecules; NMR is the leading example.^{2–9} The NMR experiments are similar in concept to fluorescence quenching experiments except that the resolution is limited only by the number of distinctly resolved nuclear resonances provided by the molecule. The change in the nuclear spin relaxation times induced by a paramagnetic cosolute may be related to the

probability that the paramagnetic cosolute contacts the particular observed nuclear spin. We extend this general approach in the present work to take advantage of specific relaxation properties of the paramagnetic center that simplify the analysis and permit quantitative interpretation of the spin relaxation rate changes in terms of intermolecular free energy differences.

Theoretical Background

In the absence of long-lived specific binding interactions, the electron–nuclear dipole–dipole coupling between a freely diffusing electron spin and a nuclear spin is generally modulated by the relative translational diffusion of the spin-bearing molecules and by the relaxation of the electron spin. The analytical models for the spin–lattice relaxation rate constants when the length as well as the orientation of the intermoment vector may change are distinct from those for intramolecular dipolar couplings modulated by rotational diffusion. The major differences are that the spectral density functions that enter the relaxation equation are not Lorentzian, but may be considerably broader, and the distance dependence of the paramagnetic contribution to the relaxation rate constant appears to be weaker because adding all contributions involves an integration over the intermoment distance that may extend to limits of the container size, which is practically infinity on the scale of molecular dimensions. Analytical expressions for the translational contribution to the paramagnetic relaxation rate constant have been developed by Ayant, Hwang and Freed, and Freed.^{10–12} For the applications of interest here, there are two limits for the electron spin relaxation time, T_{1e} , of the freely

[†] Chemistry Department, University of Virginia.[‡] Biophysics Program, University of Virginia.[§] University of Siena.

- (1) Karplus, M. *Biopolymers* **2003**, *68*, 350–358.
- (2) De Sarlo, F.; Brandi, A.; Guarna, A.; Niccolai, N. *J. Magn. Reson.* **1982**, *50*, 64–70.
- (3) Esposito, G.; Lesk, A. M.; Molinari, H.; Motta, A.; Niccolai, N.; Pastore, A. *J. Mol. Biol.* **1992**, *224*, 659–670.
- (4) Esposito, G.; Lesk, A. M.; Molinari, H.; Motta, A.; Niccolai, N.; Pastore, A. *Biopolymers* **1993**, *33*, 839–846.
- (5) Molinari, H.; Esposito, G.; Ragona, L.; Pegna, M.; Niccolai, N.; Brunne, R. M.; Lesk, A. M.; Zetta, L. *Biophys. J.* **1997**, *73*, 382–396.
- (6) Niccolai, N.; Rossi, C.; Valensin, G.; Mascagni, P.; Gibbons, W. A. *J. Phys. Chem.* **1984**, *88*, 5689–5692.
- (7) Niccolai, N.; Lampariello, R.; Bovalini, L.; Rustici, M.; Mascagni, P.; Martelli, P. *Biophys. Chem.* **1990**, *38*, 155–158.
- (8) Niccolai, N.; Ciutti, A.; Spiga, O.; Scarselli, M.; Bernini, A.; Bracci, L.; Di Maro, D.; Dalvit, C.; Molinari, H.; Esposito, G.; Temussi, P. A. *J. Biol. Chem.* **2001**, *276*, 42455–42461.
- (9) Niccolai, N.; Spadaccini, R.; Scarselli, M.; Bernini, A.; Crescenzi, O.; Spiga, O.; Ciutti, A.; Di Maro, D.; Bracci, L.; Dalvit, C.; Temussi, P. A. *Protein Sci.* **2001**, *10*, 1498–1507.

(10) Ayant, Y.; Belorizky, E.; Alizon, J.; Gallice, J. *J. Phys. I* **1975**, *36*, 991–1004.(11) Freed, J. H. *J. Chem. Phys.* **1978**, *94*, 2843–2847.(12) Hwang, L.-P.; Freed, J. H. *J. Chem. Phys.* **1975**, *63*, 4017–4025.

diffusing paramagnetic center: (1) T_{1e} may be long as compared to the translational correlation time or the rotational correlation time of the target molecule of interest. (2) T_{1e} may be short as compared to translational diffusion correlation times. The first case is relevant to nitroxide centers and some metal centers that have been used most often in the past;^{2–9} the second is important to the present discussion where we use dioxygen as the paramagnetic relaxation agent.^{13–16} The paramagnetic contribution to the k th proton in solution originating with a dipolar coupling to the oxygen center is given by Freed:¹⁷

$$\frac{1}{T_{1k}} = \frac{32\pi}{405} \gamma_I^2 \gamma_S^2 \hbar^2 S(S+1) P \frac{N_a}{1000} \frac{[S]}{bD} \{j_2(\omega_S - \omega_I) + 3j_1(\omega_I) + 6j_2(\omega_S + \omega_I)\} \quad (1)$$

where

$$j_j(\omega) = \text{Re} \left[\frac{1 + \frac{s}{4}}{1 + s + \frac{4s^2}{9} + \frac{s^3}{9}} \right] \quad (2)$$

$$s = \left(\frac{b^2}{D} \left(i\omega + \frac{1}{T_{jS}} \right) \right)^{1/2}, \quad j = 1, 2 \quad (3)$$

$[S]$ is the concentration of the paramagnetic molecule, while S is the electron spin quantum number which is 1 for oxygen, ω is the Larmor frequency for the nuclear spin I , or the electron spin S , P is a factor discussed below that equals 1 for a nonbonded hydrogen atom, b is the distance of closest approach between the electron and nuclear spin, and D is the relative diffusion constant. T_{jS} is the electron spin–lattice or transverse relaxation time for $j = 1$ or 2, respectively, and the other symbols have their usual meaning. The electron relaxation time constant for dioxygen is 7.5 ps,¹⁸ so that the magnetic relaxation dispersion is approaching the limit of Lorentzian where the correlation time for the electron–nuclear coupling is dominated by the short electron T_1 . Because the correlation time for the electron–nuclear coupling is short and remarkably insensitive to solution viscosity, the paramagnetic contribution to the spin relaxation rate constant at each proton is proportional to $P[S]$, which may also be regarded as the effective concentration of the paramagnetic molecules. Nevertheless, the relaxation efficiency depends on the intermoment distance as shown in Figure 1, where we set the correlation time at 7.5 ps, the translational diffusion constant to that of the solvent water, $2 \times 10^{-5} \text{ cm}^2 \text{ s}^{-1}$, and assume the spherical symmetry of a hydrogen atom. The calculation is truncated at distances below the sum of the van der Waals radii of the hydrogen and oxygen atoms. The dashed line indicates the relaxation rate that would be observed if the distance of closest approach to the hydrogen atom is increased by the presence of an intervening water molecule; the relaxation rate constant falls by nearly a factor

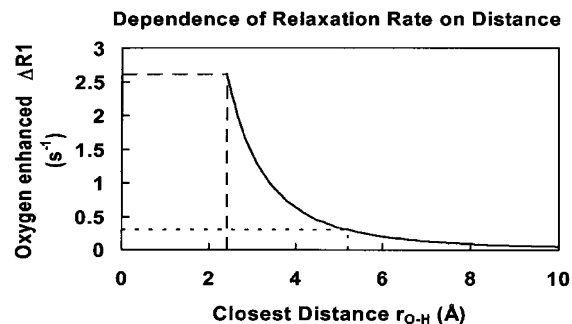


Figure 1. Proton spin–lattice relaxation rate contribution from oxygen at a magnetic field of 11.74 T computed using the Freed model¹⁷ as a function of the intermoment distance assuming a correlation time of 7.5 ps appropriate for the oxygen electron T_1 . The dotted line represents the relaxation rate at the intermoment separation of the van der Waals contact plus 3 Å, which is appropriate for the case of a proton relaxed by oxygen with an intervening water molecule separating the oxygen from the proton.

of 10 if water is in the way, which increases the intermoment separation by approximately 3 Å. Because the correlation time is the electron T_1 of oxygen, the relaxation rate constant is not significantly sensitive to changes in the translational mobility of the oxygen in the vicinity of the cosolute that is observed in the NMR spectrum. Therefore, the paramagnetic contribution to the proton relaxation rate is an effective measure of the time-average proximity of oxygen to the measured proton. For the spectrum to be in the fast chemical exchange limit, the time scale for the averaging process must be on the order of the relaxation time for the proton when the oxygen is adjacent to the proton, which is approximately 0.2 ms. All present evidence indicates that the mean lifetimes for the oxygen interactions are short as compared to this value; that is, the NMR spectrum is in the rapid exchange limit.

The parameter P includes factors that may change the accessibility to a particular nuclear spin including steric factors and any biases in the effective local concentration created by the local energetic profile. This factor may be divided into two parts: a steric factor and an equilibrium constant that accounts for locally different concentrations of the diffusing paramagnet created by the sum of intermolecular interactions. Thus, we may write for the k th proton site of the solute molecule,

$$P_k = f_k K_k \quad K_k = [\text{O}_{2,\text{local}}]/[\text{O}_{2,\text{bulk}}] \quad (4)$$

where f_k is a geometric factor that accounts for the local bonding pattern in the molecule that limits uniform access to the detected nuclear spin.

The possibility that an intermolecular complex forms raises the question of whether the relaxation equation for translational diffusion is appropriate to describe the nuclear spin relaxation. However, for oxygen, the electron spin–lattice relaxation time is very short and dominates the correlation time for the electron–nuclear dipole–dipole coupling. As a consequence, the magnetic relaxation dispersion predicted by eq 1 is Lorentzian, and essentially degenerate with that for a rotationally correlated model. In either the rotational or the translational case, the electron relaxation time is the shortest correlation time in the problem. Thus, we may treat the data without implicit bias in the relaxation model using eq 1 because the short correlation time of the oxygen decouples the relaxation efficiency from the translational or rotational dynamics of the electron–nuclear

- (13) Teng, C. L.; Bryant, R. G. *J. Am. Chem. Soc.* **2000**, *122*, 2667–2668.
 (14) Prosser, R. S.; Luchette, P. A.; Westerman, P. W.; Rozek, A.; Hancock, R. E. *Biophys. J.* **2001**, *80*, 1406–1416.
 (15) Prosser, R. S.; Luchette, P. A.; Westerman, P. W. *Proc. Natl. Acad. Sci. U.S.A.* **2000**, *97*, 9967–9971.
 (16) Hernandez, G.; Teng, C. L.; Bryant, R. G.; LeMaster, D. M. *J. Am. Chem. Soc.* **2002**, *124*, 4463–4472.
 (17) Freed, J. H. *J. Chem. Phys.* **1978**, *68*, 4034–4037.
 (18) Teng, C. L.; Hong, H.; Kiihne, S.; Bryant, R. G. *J. Magn. Reson.* **2001**, *148*, 31–34.

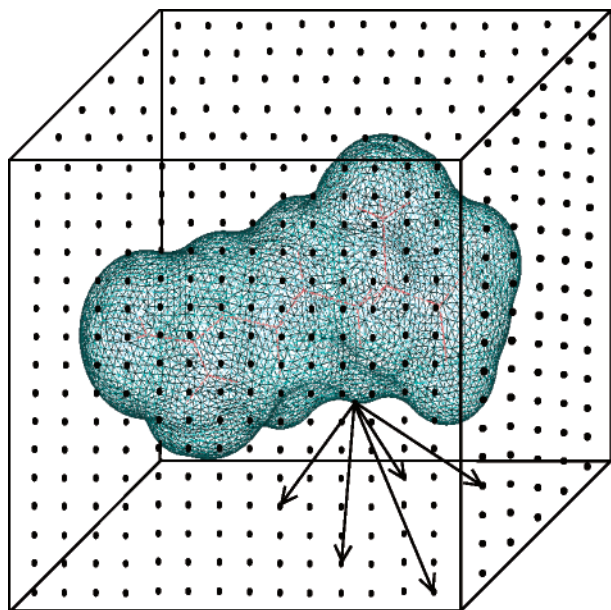


Figure 2. Lattice model diagram for computing the paramagnetic contribution to the proton spin–lattice relaxation rate in solutions where the T_1 for the paramagnetic center is short as compared to the correlation time for relative translational motion of the electron–nuclear pairs. The total paramagnetic contribution is proportional to the sum of the inverse sixth power of the distance from each point weighted by the volume element size, setting to zero any point inside an atom or the surface described by the distance of closest approach between solute protons and oxygen.

coupling. Because the paramagnetic relaxation contribution is decoupled from the translational and rotational dynamics of the interacting particles, we may compute the paramagnetic contribution to the relaxation rate by adding contributions from all points in the space available to the paramagnetic center using a lattice model. The approach is justified provided that the oxygen is uniformly distributed in the solution. As shown in Figure 2, we place a lattice of points around the solute molecule and compute the total paramagnetic contribution to the relaxation rate constant as a sum of contributions proportional to the inverse sixth power of the distance from each point weighted by the volume element size, setting to zero any point that is inside a solute atom or inside the surface described by the shortest distances of approach between oxygen and the solute atoms. This calculation agrees well with the paramagnetic contribution to proton spin–lattice relaxation rates measured in nonaqueous solutions and incorporates the several aspects of excluded volume and steric factors associated with the anisotropy in the distances of closest approach between the solute protons and the oxygen molecule.¹⁹ The steric factors for each proton observed are summarized in Table 1, where each entry is normalized to the lattice sum for a hydrogen atom, which is taken as the reference. The factors may vary by a few percent depending on the particular conformation of the molecule, but on average are about a factor of 2 reduction relative to a nonbonded hydrogen atom. The calculation yields the nuclear spin–lattice relaxation rate constants appropriate to the force-free or hard-sphere limit for the intermolecular potential.

Simultaneous measurement of the paramagnetic contribution to the solute and the solvent protons provides a simple means

Table 1. Geometric Factors Computed Relative to Hydrogen Atom Based on Lattice-Sum Ratios Obtained with a 0.025 Å Lattice Spacing

proton	fg (H)	proton	fg (H)
water	0.59	PHE:HB2	0.59
hydrogen atom	1.00	PHE:H4	0.74
DMSO	0.44	PHE:H24	0.46
ALA:HA	0.55	PHE:H42	0.57
ALA:HB1	0.68	PHE:H35	0.73
ALA:HB2	0.64	PHE:H53	0.75
ALA:HB3	0.64	TYR:HA	0.61
ARG:HA	0.52	TYR:HB1	0.54
ARG:HB1	0.50	TYR:HB2	0.60
ARG:HB2	0.41	TYR:H26	0.46
ARG:HD1	0.63	TYR:H35	0.68
ARG:HD2	0.51	TYR:H53	0.66
ARG:HG1	0.47	TYR:H62	0.57
ARG:HG2	0.40	GLU_B:HO1	0.81
LYS:HA	0.49	GLU_B:HO2	0.68
LYS:HB1	0.49	GLU_B:HO3	0.68
LYS:HB2	0.51	GLU_B:HO4	0.67
LYS:HD1	0.53	GLU_B:HO6	0.78
LYS:HD2	0.60	GLU_B:H1	0.54
LYS:HE1	0.63	GLU_B:H2	0.44
LYS:HE2	0.65	GLU_B:H3	0.51
LYS:HG1	0.46	GLU_B:H4	0.40
LYS:HG2	0.50	GLU_B:H5	0.44
PHE:HA	0.61	GLU_B:H6	0.63
PHE:HB1	0.54	GLU_B:H7	0.59

for eliminating the effects of small differences in the oxygen concentration between samples. The ratio of the paramagnetic relaxation rates may be written

$$\left(\frac{R_{1,\text{solute}}^{\text{para}}}{R_{1,\text{solvent}}^{\text{para}}}\right)_k = \frac{P_{\text{solute}}B(\omega)[\text{O}_2]_{\text{BULK}}}{P_{\text{solvent}}B(\omega)[\text{O}_2]_{\text{BULK}}} = K_k \frac{f_{k,\text{solute}}}{f_{\text{solvent}}} \quad (5)$$

where the factors f_k are the steric factors deduced from the lattice-sum calculations for the solvent protons and each solute proton, k , and $B(\omega)$ collects the remaining factors in eq 1. Thus, the paramagnetic contribution to the relaxation rate provides K_k , a measure of the concentration of the oxygen molecule at the k th proton of the solute as compared to the bulk solvent, which is taken as the appropriate reference state. The K_k values are then related to the free energy difference between the aqueous pool and that immediately adjacent to the observed solute proton by the classic relation

$$\Delta G_k^\circ = -RT \ln K_k \quad (6)$$

Experimental Section

D-Glucose, L-phenylalanine, L-arginine, L-alanine, L-leucine, L-lysine, and L-thyrosine were purchased from Sigma-Aldrich and used without further purification. The glucose and amino acid solution concentration was 50 mM with 99.96% D deuterium oxide and 99.96% deuterated DMSO (Cambridge Isotope Laboratories, Inc., Andover, MA) as solvents depending on the experiment.

Although oxygen is a convenient paramagnetic reagent, the solubility is low (~ 0.23 mM)²⁰ when equilibrated with air at 25 °C. To achieve the desired dynamic range in the relaxation measurements, all of the samples were equilibrated with 11 atm of O_2 using pressure/vacuum valve sample tubes 524 PP purchased from Wilmad Glass, Buena, NJ.

Pressure is applied to the NMR sample tubes by first clearing any dissolved air in the solution using freeze–pump–thaw cycles and then by equilibrating the protein solution with 11 atm oxygen (99.997%,

(19) Martini, S.; Teng, C.-L.; Diakova, G.; Bryant, R. G., unpublished results.

(20) Wilhelm, E.; Battino, R.; Wilcock, R. J. *Chem. Rev.* **1977**, *77*, 219–262.

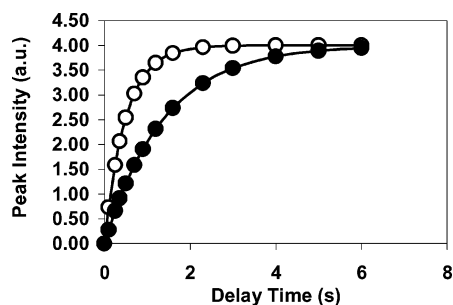


Figure 3. Representative relaxation data obtained at a proton Larmor frequency of 500 MHz for the H5 α proton of glucose under 11 atm of nitrogen (●) and 11 atm of oxygen (○).

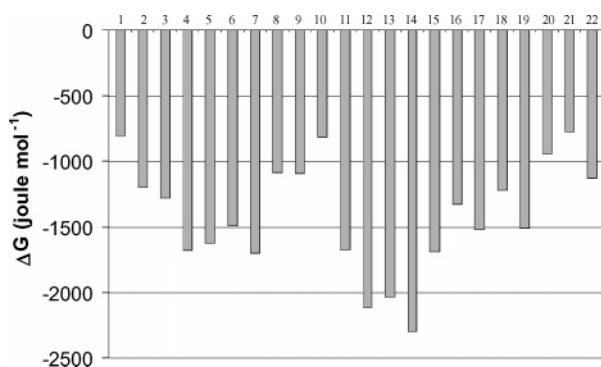


Figure 4. Free energy differences measured at individual protons for aqueous solutions of several amino acids using the lattice-sum hard-sphere model as the reference for the rates computed according to the Freed model:¹⁷ alanine, 1(H α), 2(CH₃); tyrosine, 3(H α), 4(H β 1), 5(H β 2), 6(H δ ,2), 7(H δ ,3); phenylalanine, 8(H β 1), 9(H β 2), 10(H δ ,2), 11(H δ ,3), 12(H α), 13(H α); lysine, 14(H α), 15(H ϵ), 16(H δ), 17(H γ), 18(H β); arginine, 19(H α), 20(H β), 21(H γ), 22(H δ).

BOS Gases, Murray Hill, NJ) or nitrogen (99.9995% BOS Gases, Murray Hill, NJ). Eight freeze–pump–thaw cycles were conducted, using dry ice–2-propanol as the cooling agent. Samples were sealed with a gastight screw that was further secured mechanically with Parafilm.

All NMR data were acquired using a 500 MHz Varian Unity Plus spectrometer. ¹H NMR spectra were acquired at 30 °C with spectral width of 5000 Hz. Proton spin–lattice relaxation rates were measured using the inversion recovery sequence (180– τ –90– t)_n, using a saturation recovery delay list of 0.10, 0.25, 0.36, 0.50, 0.70, 0.90, 1.20, 1.60, 2.30, 3.0, 4.0, 5.0, and 6.0 s. Each acquisition consisted of 32 transients, containing 8192 complex points. Because the recovery of proton longitudinal magnetization after a 180° pulse is not generally represented by a single exponential, due to the sum of different relaxation terms, the spin–lattice relaxation rates were calculated using the initial slope approximation, and, subsequently, a three-parameter exponential regression analysis of the longitudinal recovery curves was performed.

Results and Discussion

The paramagnetic contributions to the proton relaxation rates of solute protons were isolated by measuring the spin–lattice relaxation rate constant under 11 atm of nitrogen and 11 atm of oxygen. Representative relaxation data are shown in Figure 3 for glucose H-5 α . Figure 4 summarizes the relaxation data obtained for aqueous solutions of several amino acids utilizing the analytical approach outlined above. The free energies deduced are all negative relative to the hard-sphere model reference, but there are reproducible differences between different positions in these molecules.

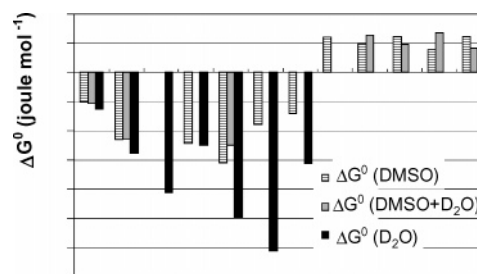


Figure 5. Free energy differences measured at individual protons for solutions of glucose in D₂O and wet dimethyl sulfoxide using the lattice-sum hard-sphere model as the reference for the rates computed according to the Freed model.¹⁷

Averaged over all of the protons measured, the free energy changes are approximately -1.4 kJ/mol, which indicates that the local oxygen concentration is approximately 80% higher than expected based on a hard-sphere model, that is, one that neglects any intermolecular association that may be driven by London dispersion forces or solvent effects. As sensed at any individual proton, these energy changes are small, approximately -0.6 in units of RT , but are easily measured. The total oxygen interaction with a particular molecule is the sum of such individual contributions; the total intermolecular free energy thus scales with the size of the solute molecule. It is important to point out that in nonpolar nonaqueous solvents such as chloroform, free energy differences such as those measured here are often essentially zero; that is, the measured equilibrium constant is 1, and the hard-sphere calculation reproduces the observation reliably.²¹ Thus, the free energy differences reported here are determined in large measure by the solvent water. Because the CH proton regions of the solute molecules are hydrophobic, and oxygen is hydrophobic and sparingly soluble in water, the unfavorable solvation of both the oxygen and the CH regions of the cosolute may be minimized by an association. We note that the formation of a clathrate structure about hydrophobic regions of the solute molecules, methyl groups, for example, that would exclude paramagnetic oxygen would lead to a measured relaxation rate constant that is smaller than expected based on a free diffusion model. In this case, the analytical strategy employed would yield a positive free energy for the oxygen–solute interaction, which is not observed in the amino acids studied here.

Glucose provides both similarities and differences as summarized in Figure 5. The CH regions of glucose uniformly show negative free energies for the oxygen interaction. In water, the average free energy difference is -1.7 kJ/mol or -0.7 in units of RT . These free energy differences are similar to those found for the CH positions in the aqueous amino acid solutions, even though the glucose is rich in OH functions that could dominate the local interactions with water. Glucose was studied in DMSO solutions so that the OH protons could be readily detected. In DMSO, and DMSO to which a small amount of deuterated water (~ 300 mM) is added, the free energy differences observed at the CH protons are smaller than those in the aqueous solutions. This significant decrease is consistent with other results in nonaqueous solutions.²¹

The OH protons detected in DMSO and wet DMSO solutions all show a positive free energy difference based on the paramagnetic relaxation rate changes. The magnitude of the free

(21) Fumino, K.; Diakova, G.; Bryant, R. G. Unpublished results.

energy change is not strongly dependent on the addition of enough water to provide one water molecule for each OH function, which implies that these effects are dominated by DMSO and not by adventitious water. The positive free energy means that the effective local oxygen concentration at the OH proton is smaller than that expected based on a free diffusion hard-sphere model. This result is consistent with partial solvent exclusion of the oxygen by hydrogen bond formation with the OH groups. The net effect is small, but clearly observable, and corresponds to approximately a 20% reduction in the effective contact concentration of oxygen.

Conclusion

The measurement of paramagnetic relaxation rate contributions from a freely diffusing paramagnetic molecule with a short electron spin–lattice relaxation time provides a direct measure of intermolecular proximity in solutions with a molecular resolution limited by the number of observable nuclear spin resonances in the solute molecule explored. The computation of the expected relaxation efficiency based on a noninteraction

or hard-sphere model provides a reference against which intermolecular free energy values may be deduced at various positions in the solute molecule studied. The intermolecular free energies that this approach provides are small, on the order of RT measured at any particular proton position in the solute, but provide a sensitive approach for exploring the average structure in the solution that is affected by all intermolecular interactions such as solvent hydrogen bonding, ionic equilibria, electrostatic effects, and secondary intermolecular association reactions. These approaches should provide considerable detail for examination of factors that control molecular recognition.

Acknowledgment. This work was supported by the National Institutes of Health, GM34541, EB002054, and the University of Virginia. We gratefully acknowledge the assistance of Dr. Brian Hinderleiter with the lattice-sum program, helpful discussions with Professors David Cafiso, Rodney Biltonen, and Jack Freed, and the technical assistance of Galina Diakova.

JA0462528